Determination of the Spatial Orientation of Objects in Automated Production

Rahim Mammadov[0000-0003-4354-3622], Timur Aliyev[0000-0001-9347-3904]

Azerbaijan State Oil and Industry University, "Instrumentation engineering" department, professor, Baku, Azerbaijan
rahim1951@mail.ru, a_tima1@mail.ru

Abstract. At present, industrial enterprises manufacture products with a constantly changing nomenclature by introducing robotic systems with elements of artificial intelligence into the production process. The latter allow to increase productivity in conditions when it is difficult or impossible for a person to perform certain production operations.

The most important stages of production where industrial robots need to be used are the processing of workpieces and their assembly. At these stages, the workpieces must enter the working area in strict sequence, at the right time and place, and in a certain position.

However, in the process of delivery of details, changes are possible, which leads to the need to use identification systems. Mechanical systems have proven themselves very well, however they are very cumbersome and difficult to maintain.

The use of systems of technical vision, which allows for the recognition and spatial orientation of an object, seems promising. The study is carried out on the basis of the system of three equations obtained by the authors, showing the dependence of the change in the moments of inertia of a plane figure during its triple rotation in space.

Triple rotation means the rotation of an object around three mutually perpendicular coordinate axes OX, OY and OZ at certain angles α, β and γ, respectively.

By solving the system of equations for the variables α, β and γ, one can determine the spatial orientation of the object.

The obtained theoretical results were verified by computer modeling of the proposed method for determining the position of spatial objects. The experiments were carried out on four reference images, which are rotated in space at arbitrary angles.

The simulation results showed that the proposed system of equations showing the dependence of the change in the moments of inertia of a plane figure during its triple rotation in space is valid for each rotated image.

This approach can be used in flexible automated production to clarify the spatial position of workpieces entering the working area of a processing or assembly machine.

Keywords: industrial robots, recognition object, object features, inertia moment

1 Introduction

The application of artificial intelligence technology in robot systems enables to increase the efficiency by adapting to constant changes in the working condition and to achieve greater manufacturing flexibility [1, 2]. Intelligent multi-robot systems are in demand first of all for the work in restricted access conditions and when there is a need for effective decision making with minimal human operator participation [3, 4].

Contemporary robot systems are widely used in industrial production [5, 6]. They have great functional flexibility thanks to progressive actuating mechanism, microprocessor control systems with developed software, vision and other sensors, adaptive capabilities, and can replace people in the implementation of various types of operations [7, 8]. In addition, computer-aided systems are actively used in the food industry for sorting food products [9].

2 Problem statement

One of the general purpose systems of intelligent robots are technical vision systems [10, 11]. They solve such problems as finding the research object, identifying it, determining its coordinates on the location in the manipulator working area, geometric parameters of the object to ensure its capture, and also industrial assembly and quality control [4, 9].

In the process of manufacturing the product, the main purpose of industrial robots is the installation of pre-oriented storage in the working area of the machine and the removal of completed parts from the machine with subsequent installation on a conveyor line. The parts are delivered only sequentially to the assembly area, i.e., at the right time and place [12, 13].

However, during transportation from one working area to another one, as a result of the influence of external factors, changes in the spatial orientation of products are possible. In this regard, it is promising to make identification of blanks at each stage of processing.

Currently, a number of methods have been developed for the recognition spatial images of objects, however, each of them has its faults. So, in [11], parallel transformation and rotation of the image being a special case of spatial displacements are studied. In [14, 15] the analysis is carried out on reference points, numbering of which remains constant for spatial distortions, which is not always achievable. In [16,17], image analysis is carried out along the contour, which is the most sensitive to distorting factors. In [18], moments of inertia are considered as the main features, however, an analysis of the properties of moments of inertia showed that the features, in this case, are integral for a wide range of objects, which makes it difficult to recognize objects of one cluster.

The process of recognizing a spatial object on images is significantly complicated by the change in all geometric features. This is due to the image undergoing such distortions as rotation and shear. Thus, it can be said that, the task of identifying features being invariant to spatial distortions of object images has not been solved completely.

3 Problem solving method

In this article, statistical moments are proposed to be used as reference points for the image, and on the basis of this principle, an effective methodology for determining the orientation of objects in space has been developed.

One of the methods for recognizing the object located arbitrarily in space is the recognition of two-dimensional images of its sides by comparing them with reference images.

As a matter of fact, the side image of the object is a flat closed single-contour or multi-contour figure. Thus, the process of recognizing the object located arbitrarily in space can be reduced to the recognition of several plane figures located arbitrarily in space. If the flat figure is a solid body, then the analysis of its position in space can be made by analyzing the position of the fixed marker point located on a flat figure. In this case, arbitrary location of the plane figure, and consequently, a marker point in space, is considered as the rotations of the plane figure around three coordinate axes. The analysis of the plane figure position will be carried out by analyzing the position of the marker point projection on the frontal plane. In this case, the origin point is located in the center of the plane figure.

In the course of the research [19], the authors obtained the dependence of the change in the coordinates of the marker point projection during the rotation of the frontal plane around the horizontal axis OX, followed by rotation around the vertical axis OY:

$$x_2 = x_0 \cdot \cos\beta, \tag{1}$$

$$y_2 = y_0 \cdot \cos\alpha \pm x_0 \cdot \sin\beta \cdot \sin\alpha, \tag{2}$$

where x_0, y_0 are the coordinates of the marker point on the initial frontal plane; x_2, y_2 are the coordinates of the marker anguish after its double rotation; α is the rotation angle around the horizontal axis; β is the rotation angle around the vertical axis.

After integrating expressions (1) and (2) for all figures, the inertia moment of the plane figure is obtained after its double rotation in space:

$$J_{X2} = \cos^3\alpha \cdot \cos\beta \cdot J_{X0} \pm 2 \cdot \cos^2\alpha \cdot \sin\alpha \cdot \sin\beta \cdot \cos\beta \cdot J_{X0Y0} + \\ + \cos\alpha \cdot \sin^2\alpha \cdot \cos\beta \cdot \sin^2\beta \cdot J_{Y0}, \tag{3}$$

$$J_{Y2} = \cos\alpha \cdot \cos^3\beta \cdot J_{Y0}, \tag{4}$$

$$J_{X2Y2} = \cos^2\alpha \cdot \cos^2\beta \cdot J_{X0Y0} \pm \cos\alpha \cdot \sin\alpha \cdot \cos^2\beta \cdot \sin\beta \cdot J_{Y0}, \tag{5}$$

where J_{X0}, J_{Y0}, J_{X0Y0} are respectively the inertia moment of the initial figure along the axis OX, OY and the centrifugal inertia moment; J_{X2}, J_{Y2}, J_{X2Y2} are respectively the inertia moment of the plane figure after its double rotation in space, along the axis OX, OY and the centrifugal inertia moment.

As it is known [20], the inertia moment of the section during the rotation of the axes passing in the plane of the section around the axis passing perpendicular to the plane of the section are related by equations (6) ÷ (8):

$$J_U = J_X \cdot \cos^2\gamma + J_Y \cdot \sin^2\gamma - J_{XY} \cdot \sin 2\gamma , \tag{6}$$

$$J_V = J_X \cdot \sin^2\gamma + J_Y \cdot \cos^2\gamma + J_{XY} \cdot \sin 2\gamma , \tag{7}$$

$$J_{UV} = J_{XY} \cdot \cos 2\gamma + \frac{J_X - J_Y}{2} \cdot \sin 2\gamma , \tag{8}$$

where J_X, J_Y, J_{XY} are axial and centrifugal inertia moments of the section with respect to the initial axes; J_U, J_V, J_{UV} are axial and centrifugal inertia moments of the section with respect to the rotated axes; $\gamma\gamma$ is rotation angle.

Substituting expressions (3) ÷ (5) into equations (6) ÷ (8) and denoting the constants J_U, J_V, J_{UV} respectively, as, J_{X3}, J_{Y3}, J_{X3Y3} the dependence of the change in the inertia moments of the plane figure is obtained during its triple rotation in space:

$$J_{X3} = f(\alpha, \beta, \gamma, J_{X0}, J_{Y0}, J_{X0Y0}) , \tag{9}$$

$$J_{Y3} = f(\alpha, \beta, \gamma, J_{X0}, J_{Y0}, J_{X0Y0}) , \tag{10}$$

$$J_{X3Y3} = f(\alpha, \beta, \gamma, J_{X0}, J_{Y0}, J_{X0Y0}) . \tag{11}$$

As a result, a system of three equations with three variables is obtained: α, β and γ. Solving the system of equations (9) ÷ (11), the position of the object side in space, and, consequently, the position of the object itself can be found.

4 Computer Simulations

In order to check the obtained theoretical results, computer simulation was carried out.

For a more detailed analysis of the proposed methodology, it is desirable to study objects belonging to the same cluster, but significantly differing in form. As a feature characterizing the shape of the object was chosen "shape indicator" defined by the expression [21]:

$$\rho = \frac{\text{Perimeter}^2}{\text{Area}} \tag{12}$$

Studies have shown that for real parts produced by flexible automated manufacturing, the shape index does not exceed 80. Therefore, abstract images were used in computer modeling. To simplify, stylized animal figures were chosen as images of the object.

Figure 1 presents four flat figures, which are the original images.

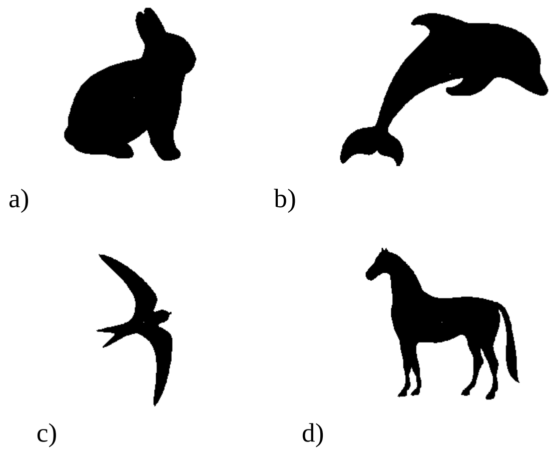

Fig. 1. Original images

Table 1 summarizes the main parameters of these figures.

Table 1. Parameters of original images

Figure	Object height, pixel	Object width, pixel	Object area, pixel	Object shape indicator (ρ).
Fig. 1,a.	254	214	30211	41
Fig. 1,b.	254	356	30718	79
Fig. 1,c.	254	123	8766	119
Fig. 1,d.	254	201	23992	160

At the first stage, using the AutoCAD system, the original images were rotated in the image plane at angles γ in increments equal to 40º (40º; 80º; 120º; 160º; 200º; 240º; 280º; 320º). As a result, 8 new images were obtained. Further, the moments of inertia (J_{X3_meas}, J_{Y3_meas}, J_{XY3_meas}) were measured for the obtained images. In addition, using the formulas (9)÷(11), the moments of inertia (J_{X3_calc}, J_{Y3_calc}, J_{XY3_calc}) were calculated for the image data, where α=0 and β=0. The relative divergences (D) between the corresponding moments of inertia were also calculated:

$$D_X = \frac{\left|J_{X3\_meas} - J_{X3\_calc}\right|}{J_{X3\_meas}};\ D_Y = \frac{\left|J_{Y3\_meas} - J_{Y3\_calc}\right|}{J_{Y3\_meas}};\ D_{XY} = \frac{\left|J_{XY3\_meas} - J_{XY3\_calc}\right|}{J_{XY3\_meas}}. \quad (13)$$

Figure 2 presents the graphs of the dependence of relative divergences D on the rotation angle γ for the moments of inertia J_{X3}, J_{Y3}, J_{XY3}, respectively.

At the second stage, using the AutoCAD system, the original images were rotated around the horizontal axis at angles α in increments equal to 10º (10º; 20º; 30º; 40º; 50º; 60º; 70º; 80º). As a result, 8 new images were obtained. Further, similarly to the first stage, moments of inertia were measured for the obtained images (J_{X3_meas}, J_{Y3_meas}, J_{XY3_meas}), according to formulas (9)÷(11), moments of inertia (J_{X3_calc}, J_{Y3_calc}, J_{XY3_calc}) were calculated for these images, where β=0 and γ=0, and according to formulas (13), the relative divergences (D) between the corresponding moments of inertia were calculated.

Figure 3 presents graphs of the dependence of the relative divergences D at rotation angle α for the moments of inertia J_{X3}, J_{Y3}, J_{XY3}, respectively.

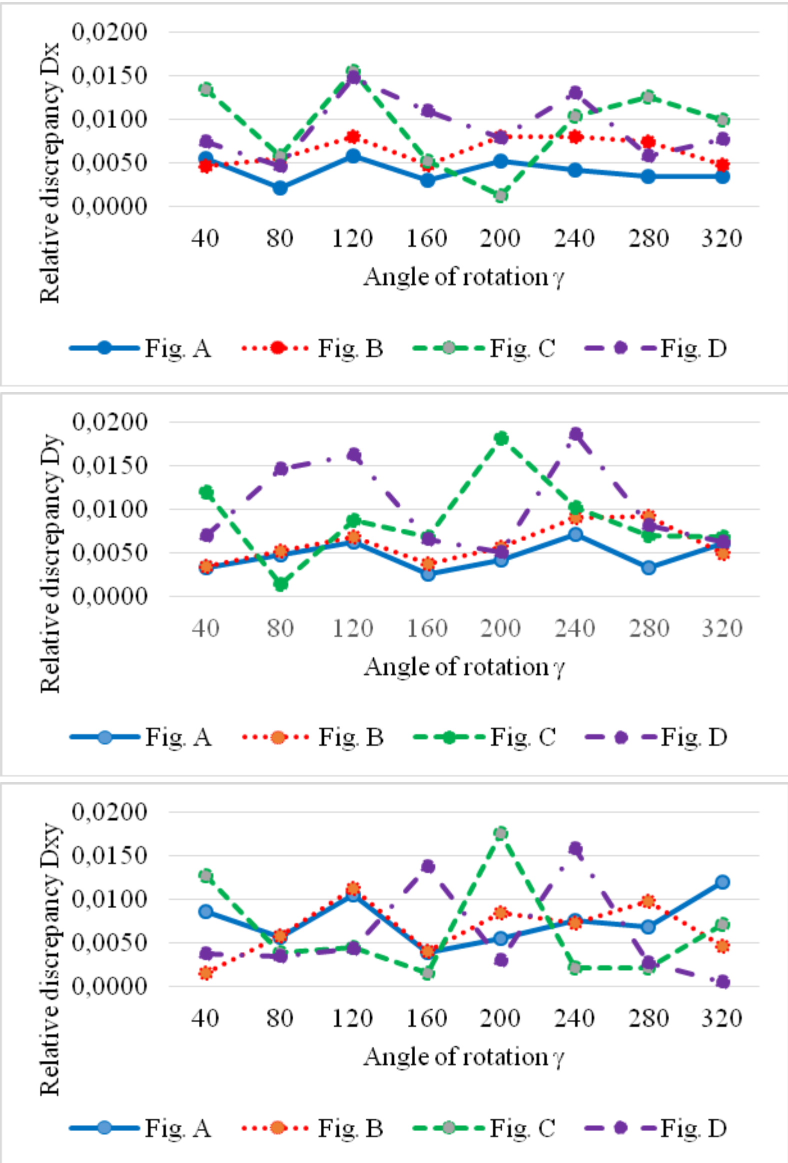

a) b) c)

Fig. 2. The dependence of the relative divergences between the corresponding moments of inertia at angles of rotation of the object in the image plane

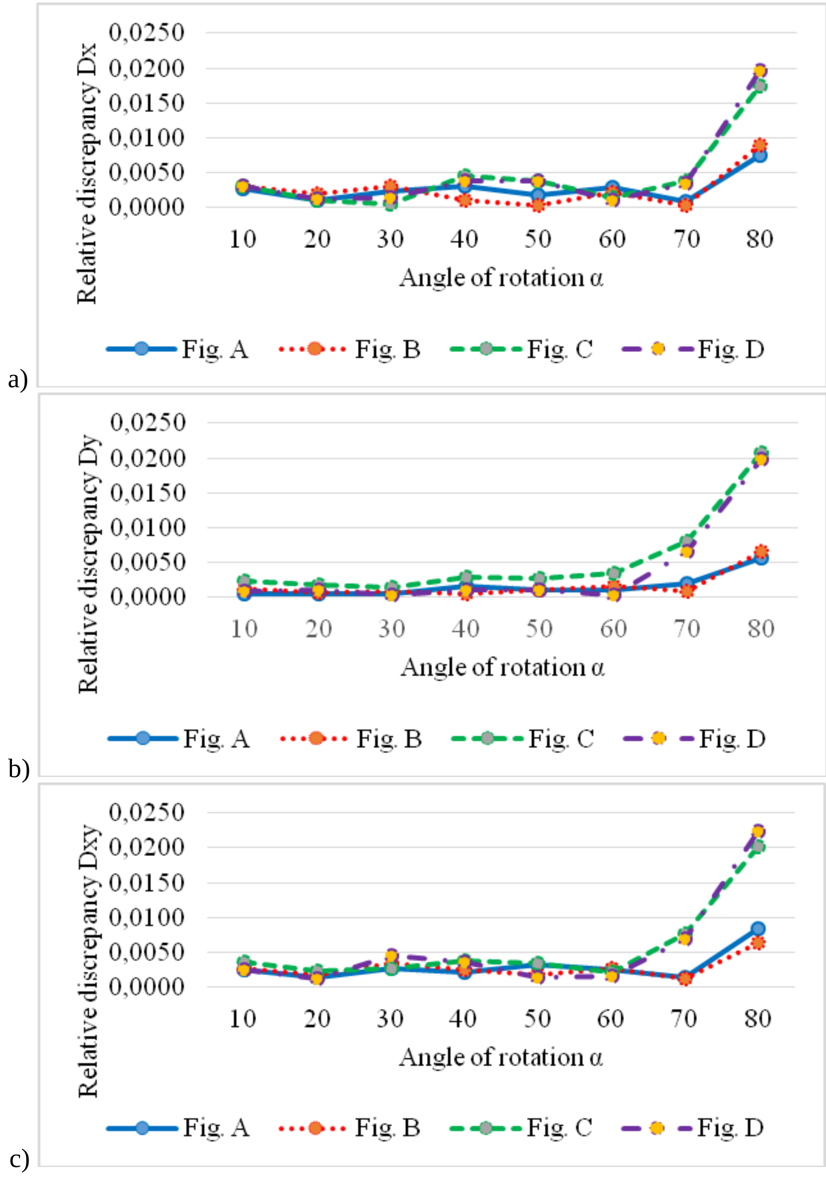

Fig. 3. The dependence of the relative divergence between the corresponding moments of inertia at angles of rotation of the object around the horizontal axis

At the third stage, using AutoCAD system, the original images were rotated around the vertical axis at β angles in increments equal to 10º (10º; 20º; 30º; 40º; 50º; 60º; 70º; 80º). As a result, 8 new images were obtained. Further, similarly to the first stage, moments of inertia were measured for the obtained images ((J_{X3_meas}, J_{Y3_meas}, J_{XY3_meas}); according to formulas (9)÷(11), the moments of inertia (J_{X3_calc}, J_{Y3_calc},

J_{XY3_calc}) were calculated for these images, where α=0 and γ=0; using the formulas (13), the relative divergences (D) between the corresponding moments of inertia were calculated. Figure 4 presents the graphs of the dependence of the relative divergence D on the rotation angle β for the moments of inertia J_{X3}, J_{Y3}, J_{XY3}, respectively.

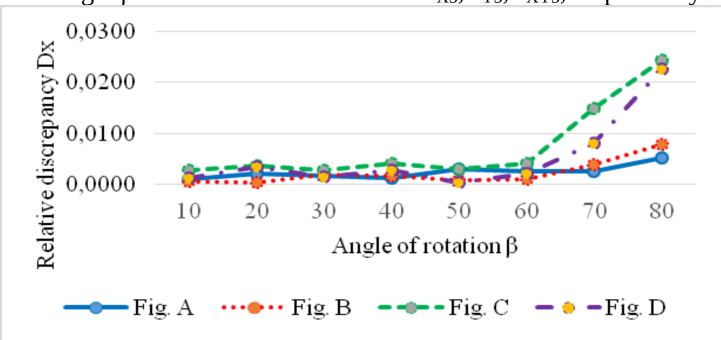

a)

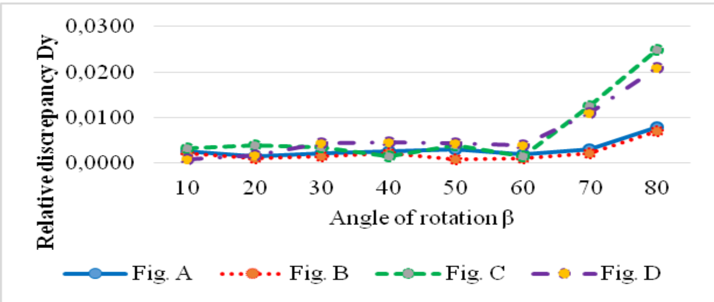

b)

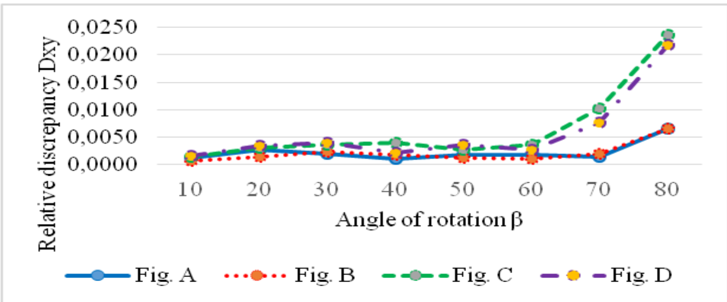

c)

Fig. 4. The dependence of the relative divergence between the corresponding moments of inertia at angles of rotation of the object around the vertical axis

At the fourth stage, using the AutoCAD system, the original images were rotated in the image plane at angles γ in increments equal to 40º, with subsequent rotations around the horizontal axis at angles α in increments equal to 10º and around the vertical axis at angles β in increments equal to 10º (10º, 10º, 40º; 20º, 20º, 80º; 30º, 30º, 120º; 40º, 40º, 160º; 50º, 50º, 200º; 60º, 60º, 240º; 70º, 70º, 280º; 80º, 80º, 320º). As a result, 8 new images were obtained. Further, similarly to the first stage, moments of inertia (J_{X3_meas}, J_{Y3_meas}, J_{XY3_meas}) were measured for the obtained images; according to the formulas (9)÷(11) the moments of inertia (J_{X3_calc}, J_{Y3_calc}, J_{XY3_calc}) were calculated for these images; using the formulas (13), the relative divergences (D) between the corresponding moments of inertia were calculated.

Figure 5 presents the graphs of the dependence of the relative divergence D at the rotation angles α, β, and γ for the moments of inertia J_{X3}, J_{Y3}, J_{XY3}, respectively.

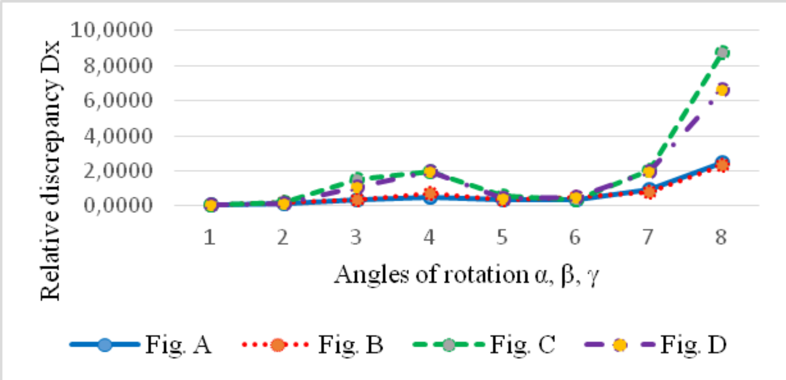

a)

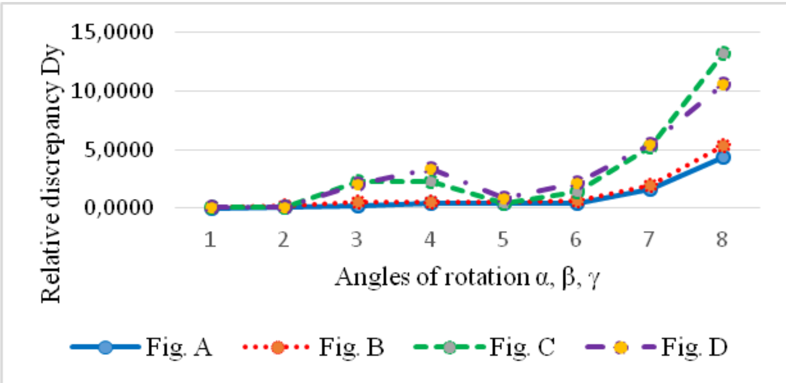

b)

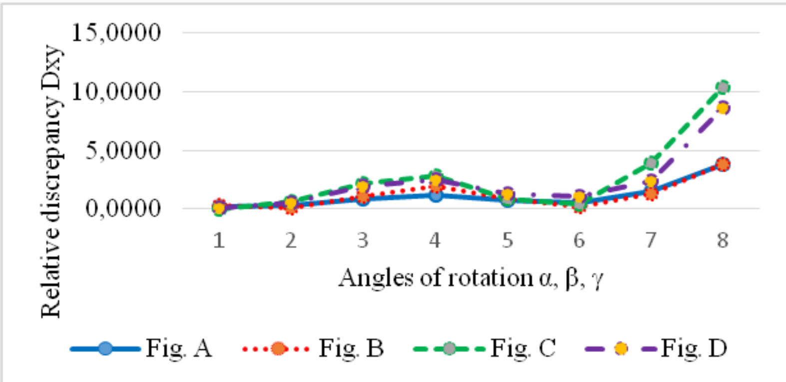

c)

Fig. 5. The dependence of the relative divergence between the corresponding moments of inertia at rotation angles of the object in the image plane, around the horizontal and vertical axes

5. Conclusions

As it can be seen from Figure 2 that the graphs are oscillatory in nature. That is, it is possible to come to such a conclusion that the angle of the object rotation in the image plane does not significantly affect the value of the divergence D, and is located in certain acceptable intervals. The reason for the dispersion of the divergence D is the appearance of distortion of discrete images with low resolution.

Additional criteria for assessing the divergence D is the shape indicator. The higher the shape indicator, the greater the dispersion of divergence. The reason for this is the distortion of the pixels of the contour of the object during rotation.

It can be seen from Figure 3 and Figure 4 that the graphs are exponential in nature. That is, it is possible to come to such a conclusion that the angle of the object rotation around the horizontal or vertical axis has a significant effect on the value of the divergence D only at its extreme values. At the same time, at small and average values, it is located in certain acceptable intervals. Similarly, additional criteria for assessing the divergence D can serve as a shape indicator. The higher the shape indicator, the greater increasing rate of the exponent. The reason for this, in addition to low resolution, it serves as the change in the image area.

As it is seen from figure 5 that the graphs are complex oscillating-exponential in nature. In this graph, the exponents have a greater speed than the graphs in figures 3 and 4. So, it is possible to come to such a conclusion that for the objects randomly located in space, the value of the divergence D will be essentially already close to the extreme values of the rotation angle. At the same time, when increasing the indicator, the graphs acquire an N-shaped form.

As it can be seen from the above-mentioned statements, taking into account the computational error, the system of equations (9) ÷ (11) is justified for each rotated image and with the exception of extreme values, it is applied to all positions of the object. Thus, using the equations obtained by the authors, the system of equilibrium dependence of the moments of inertia of the flat figure with its triple rotation in space can be carried out in parallel to the recognition and spatial orientation of the object. By means of this definition, the orientation of the object in space will be produced for a fixed time.

This equilibrium system can be used in flexible automated production to clarify the spatial position in the working area of a processing or assembly machine. Thus, it can be applied to autonomous mobile robots to search for objects in this area.

References

1. Bo-hu Li, Bao-cun Hou, Wen-tao Yu, Xiao-bing Lu & Chun-wei Yang.: Applications of artificial intelligence in intelligent manufacturing: a review. Frontiers of information technology & electronic engineering, vol. 18, pp. 86–96 (2017).
2. C. Renzi, F. Leali, M. Cavazzuti & A. O. Andrisano.: A review on artificial intelligence applications to the optimal design of dedicated and reconfigurable manufacturing systems. The International Journal of Advanced Manufacturing Technology, vol. 72, pp. 403–418 (2014).

3. Crisan N., Pop I. & Coman I.: Robotic Surgical Approach in Limited Access Anatomical Areas. New Trends in Medical and Service Robots. Assistive, Surgical and Educational Robotics. Mechanisms and Machine Science, 38, pp.165-177 (2016).
4. Gerlind Wisskirchen, Blandine Thibault Biacabe et al.: Artificial intelligence and robotics and their impact on the workplace. IBA Global Employment Institute. (2017).
5. Alp Ustundag, Emre Cevikcan.: Industry 4.0: Managing The Digital Transformation. Springer International Publishing, Switzerland (2018).
6. Miller M. R., Miller R. Robots and Robotics: Principles, Systems, and Industrial Applications. McGraw-Hill Education (2017).
7. Eugenio Brusa.: Mechatronics. Principles, technologies and applications. Nova Science Publishers Inc., New York (2015).
8. Héctor C. Terán, Oscar Arteaga, Guido R. Torres, A. Eduardo Cárdenas, R. Marcelo Ortiz, Miguel A. Carvajal, O. Kevin Pérez.: Mobile robotic table with artificial intelligence applied to the separate and classified positioning of objects for computer-integrated manufacturing. Russian Conference on Artificial Intelligence - RCAI 2018, pp. 218-229 (2018).
9. Caldwell D.G.: Robotics and automation in the food industry. Current and future technologies. Woodhead Publishing Limited (2013).
10. Phansak Nerakae, Pichitra Uangpairoj, Kontorn Chamniprasart.: Using machine vision for flexible automatic assembly system. International Conference on Knowledge Based and Intelligent Information and Engineering Systems, pp. 428 – 435 (2016).
11. Mamedov R.K., Mutallimova A.S., Aliyev T.Ch.: Ispol'zovaniye momentov inertsii izobrazheniya dlya invariantnogo k affinnym preobrazovaniyam raspoznavaniya. Vostochno-Yevropeyskiy zhurnal peredovykh tekhnologiy. №4/3 (58), pp. 4-7 (2012).
12. KLS Sharma.: Overview of Industrial Process Automation, second edition. Elsevier Inc. (2017).
13. Siciliano B., Khatib. O.: Springer Handbook of Robotics. 2nd edition. Springer-Verlag Berlin Heidelberg (2016).
14. Vimal Sudhakar Bodke, Omkar S.: Vaidya Object Recognition in a Cluttered Scene using Point Feature Matching. International Journal for Research in Applied Science & Engineering Technology, pp. 286-290 (2017).
15. Toshiaki Ejima, Shuichi Enokida, Toshiyuki Kouno.: 3D Object Recognition based on the Reference Point Ensemble. International Conference on Computer Vision Theory and Applications pp. 261-269 (2014).
16. Farnoosh Ghadiri, Robert Bergevin, Guillaume-Alexandre Bilodeau: Carried Object Detection Based on an Ensemble of Contour Exemplars. 14th European Conference Computer Vision – ECCV 2016. Amsterdam, October 11–14, pp. 852-866 (2016).
17. Xin Li, Fan Yang, Hong Cheng, Wei Liu, Dinggang Shen: Contour Knowledge Transfer for Salient Object Detection. 15th European Conference Computer Vision – ECCV 2018. Munich, September 8-14, pp. 370-385 (2018).
18. Mohammad Arafah, Qusay Abu Moghli.: Efficient Image Recognition Technique Using Invariant Moments and Principle Component Analysis. Journal of Data Analysis and Information Processing, pp. 1-10 (2017).
19. Mamedov R.K., Aliyev T.Ch.: Kontrol' polozheniya 3D-ob"yektov v gibkikh avtomatizirovannykh sistemakh. Povysheniye dostovernosti raspoznavaniya. – LAP LAMBERT academic publishing (2016).
20. Slocum S.E., Hancock E.L.: Text-book on the strength of materials. Revised edition. FB&c Ltd (2016).
21. Jens Feder.: Fractals. Plenum press. New York. 1988.